Thermochimica Acta 512 (2011) 98–104

Contents lists available at ScienceDirect

Thermochimica Acta

journal homepage: www.elsevier.com/locate/tca

Application of Cu-water and Cu-ethanol nanofluids in a small flat capillary pumped loop

Lin Lu, Lun-Chun Lv, Zhen-Hua Liu*

School of Mechanical Engineering, Shanghai Jiaotong University, 800 Dongchuan Road, Shanghai 200240, PR China

A R T I C L E I N F O

Article history:
Received 16 April 2010
Received in revised form 4 September 2010
Accepted 7 September 2010
Available online 21 September 2010

Keywords:
Nanofluids
Heat transfer enhancement
CPL
Heat pipe

A B S T R A C T

An experimental study was carried out to investigate the thermal performance of a flat capillary pumped loop (CPL) using the water based and the ethanol based Cu nanofluids as the working fluids under several steady sub-atmospheric operating pressures. The evaporator of the CPL was placed horizontally and heated from the bottom. The experimental results show that adding Cu nanoparticles into both base fluids can significantly enhance the evaporating heat transfer coefficient and the maximum heat removal capacity. There is an optimal mass concentration of Cu nanoparticles corresponding to the maximum heat transfer enhancement. The operating temperature or the operating temperature has an apparent effect on the heat transfer enhancement. The heat transfer enhancement effects increase distinctly with increasing the operating temperature. The heat transfer coefficient and the maximum heat removal capacity can be increased up to 45% and 16% after substituting Cu-ethanol nanofluids for the base fluids, respectively. The present investigation discovered that the thermal performance of a CPL can be evidently strengthened by using Cu nanofluids.

© 2010 Elsevier B.V. All rights reserved.

1. Introduction

The pursuit of high performance and miniaturization of electronic component in recent years leads to production of more heat per unit volume. As a result, how to dissipate the heat becomes a critical factor in the electronic product design. As a high effective heat-exchanger device, the capillary pumped loop (CPL) has attracted more and more attention.

The CPL is a two-phase thermal control system that uses capillary force formed in the vicinity of the wick surface to transport the working liquid. A large number of investigations have been conducted on the heat transfer characteristics in CPLs. The first CPL was proposed by Stenger in 1966 [1], but it received special attention in the late 1970s. At that time, CPL technology had been developed as an option for transporting thermal energy within spacecrafts and satellites [2,3]. Most of CPLs have a reservoir that is used for temperature control as well as storing excess working fluid and providing pressure priming [4]. Currently, miniaturization of CPL is at the forefront of an extensive research and development to provide cooling solution to the high load/heat flux problem of advanced electronic packaging [5]. At the same time, CPLs without the reservoir have appeared also. Chen and Lin [6] carried out a research on using the CPL without the reservoir for cooling electronic chips. This CPL without the reservoir had a flat evaporator using porous material as capillary structure. They investigated the parameters affecting the thermal performance of the CPL. Figus et al. [7] performed a research to apply the CPL for the cooling system of the print circuit board (PCB). The used CPL had a flat evaporator and had no the reservoir. Ramos and Vlassov [8] also carried out an experimental and theoretical study on thermal performance of a grooved construction CPL without the reservoir. Their study showed that the CPL without a reservoir could be used with a heat source without a precise control.

Since the heat pipe utilizes phase change of the working fluid to transfer heat, the selection of working fluid is of essential importance to achieve the maximum heat transfer. In 1995, Choi [9] firstly proposed the concept of "nanofluid". That is, adding nanoscale metal or metal oxide particles in the liquid with a certain way and proportion, which forms a new class of heat transfer and cooling working fluid. Because of its stability and high thermal conductivity, the nanofluid shows a promising prospect in the heat transfer enhancement. At present, research on the heat transfer of the nanofluid concentrate mainly on forced convection in tube and pool boiling. Keblinski et al. [10] made an interesting review to discuss the properties of nanofluids and future challenges. Wang and Mujumdar [11] summarized the recent researches on flow and forced convective heat transfer characteristics of nanofluids. Weerapun and Somchai [12] summarized the published experimental and numerical investigations of forced convective heat transfer of nanofluids. Majid and Bahrami et al. [13] provided an overview on the effective thermal conductivity of nanofluids. Cheng et al. [14] carried out an overview on the studies of nanofluids boiling and

* Corresponding author. Tel.: +86 21 34206568; fax: +86 21 34203530.
E-mail address: liuzhenh@sjtu.edu.cn (Z.-H. Liu).

0040-6031/$ – see front matter © 2010 Elsevier B.V. All rights reserved.
doi:10.1016/j.tca.2010.09.007

Nomenclature

A_e	the area of the bottom of the evaporator (m^2)
I	the current (A)
l	the effective length (m)
h	the heat transfer coefficient ($W/(m^2\,K)$)
Q	heating power (W)
Q_{loss}	heat loss (W)
q	heat flux (kW/m^2)
R	total heat resistance of CPL (K/W)
T	temperature (°C)
T_v	operating temperature, or saturated temperature of the vapor (°C)
Δ	uncertainty
V	electric voltage (V)
w	nanoparticles mass concentration (wt%)
ρ	density (kg/m^3)
θ	nanoparticles volume fraction (%)

Subscripts

0	water
c	condenser
e	evaporator
l	liquid
n	nanofluid
v	vapor
w	wick

two phase flow. Up to now, the number of published literature has reached over 200 [15].

The studies concerning application of nanofluids in heat pipes are still in its initial stage, almost all studies are experimental investigations and some experimental results cannot be unified yet. Research on the application of nanofluids in heat pipes was firstly published by Chien et al. in 2003 [16]. Over 20 relevant articles have been published since then, involving micro-grooved heat pipes [16–22], mesh wicked heat pipes [23,24], sintered metal wicked heat pipes [25–27], oscillating heat pipes [28–31] and various thermosyphon [32–39]. The nano-materials used include metals, metal oxides, diamond, carbon nanotubes and several other materials.

Because the construction and the geometrical size of heat pipes, the kind of the base liquids, the kind and size of nanoparticles and the operating conditions widely varied among these experiments. It is therefore very difficult to quantitatively make a comparison among the different experimental data. Also, most of the exiting researches proposed only some qualitative conclusions. However, the qualitative trends are the same whereby the heat transfer was enhanced by substituting nanofluids for the base fluid.

Up to now, no study concerning application of nanofluids in CPL has been reported. This study focuses on the fundamental understanding of the steady operation characteristics of a miniature CPL with a flat mesh wicked evaporator and without the reservoir after substituting the water based Cu nanofluid and the ethanol based CuO nanofluid for the base fluids as the working fluids. Effects of filling rate, kind of the base fluid, nanoparticle mass concentration and operating temperature on the evaporating heat transfer coefficient (HTC), the maximum heat removal capacity or the maximum heat flux (MHF) and the total heat resistance in the CPL were investigated and discussed. The experimental results are useful for designing miniature CPLs using nanofluids as the working liquid.

Table 1
Structural parameters of CPL system.

Evaporator	Vapor line
Outside diameter: 0.036 m Inner diameter: 0.031 m Inner height: 0.014 m Thickness of the bottom: 0.003 m	Outside diameter: 0.004 m Inner diameter: 0.003 m Length: 0.45 m
Condenser	**Liquid line**
Outside diameter: 0.004 m Inner diameter: 0.003 m Length: 0.26 m	Outside diameter: 0.004 m Inner diameter: 0.003 m Length: 0.45 m

2. Experimental apparatus and process

2.1. Experimental apparatus

Fig. 1 shows the schematic diagram of the experimental apparatus. The experimental system consisted of a test CPL, a DC power supply, a data acquisition system and a computer. The test CPL was composed of a flat evaporator, a condenser, an outlet vapor line and an inlet liquid line. The evaporator was heated by a skin heater that was mounted on the copper bottom wall of the evaporator and the input power was supplied by a DC power supply. The measured electric voltage drop across the skin heater and the current were used to calculate the heat input. The vapor in the condenser was cooled by the cooling water from a temperature-controlled water bath. All the data from thermocouples and the pressure transducer were recorded by the data acquisition system (Agilent-34970) which is fed into the computer. The temperature of the cooling water was adjusted to keep the operating pressure at a constant value for the different input power. The design characteristics of the CPL are given in Table 1.

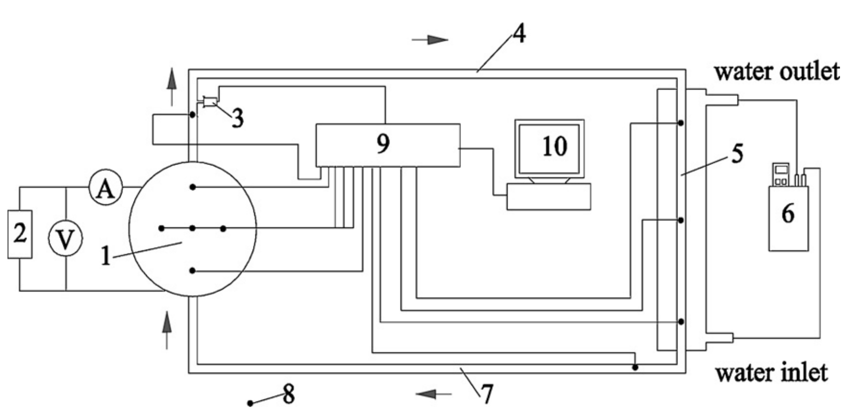

Fig. 1. Schematic diagram of experimental apparatus TEM. (1) Evaporator; (2) DC power supply; (3) pressure transducer; (4) vapor line; (5) condenser; (6) thermostat reservoir; (7) liquid line; (8) thermocouple locations; (9) digital acquisition system; (10) computer.

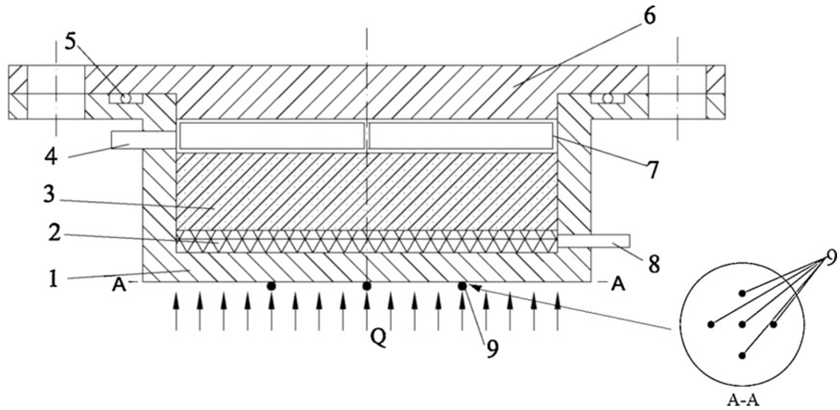

Fig. 2. Schematic diagram of the evaporator. (1) Base of the evaporator; (2) 150 meshes; (3) 300 meshes; (4) vapor line; (5) viton o-ring; (6) flange; (7) supporter of mesh; (8) liquid line; (9) thermocouple locations.

Fig. 2 shows a detailed schematic diagram of the evaporator, which was similar to one of the three classical types of evaporators mentioned by Faghri [4]. The evaporator consisted of the base, mesh screens, the supporter of the screen, the outlet vapor line, the inlet liquid line and the flange. The supporter was used to keep the mesh screens close to the wall. Two mesh layers were used in this CPL and the wicks were made of stainless steel mesh screens. The wire mesh network and the thickness of the mesh screen at the bottom were 150 and 2 mm, and, those at the top were 300 and 6 mm. The reason for choosing two sizes of mesh layers was to decrease the flow resistance of the working fluid in the mesh layers.

Ten 0.1 mm Omega thermocouples were mounted on the CPL to measure the surface temperature distribution. Five thermocouples were installed at the bottom wall of the evaporator: one was placed at the center, and the others were uniformly distributed at a radial position of 7.5 mm from the center. The thermocouple locations were shown in Fig. 2. The average wall temperature of the evaporator was the arithmetical average of the five thermocouples. Because the temperature difference between the outer wall and the inner wall was very small (less than 0.1 K), the measured average outer wall temperature was directly applied as the average inner wall temperature. One thermocouple was installed at the outlet of the evaporator to measure the saturation temperature of the vapor, i.e., the operating temperature. In addition, one thermocouple was installed at the outlet of the condenser to measure the temperature of the working liquid. The others were installed equidistantly on the condenser to measure the average wall temperature of the condenser. A pressure transducer was installed at the outlet of the evaporator to measure the saturated pressure of the vapor.

2.2. Working liquids

In the present experiment, both distilled water and chemical-pure ethanol were used as the base fluids and the nanofluids consisted of the base fluids and Cu nanoparticles. Cu nanoparticles were commercial product made by the gas condensation method. The conference average diameter reported by the maker was 20 nm. The nanofluids were prepared by directly dispersing Cu nanoparticles into the base fluids, after which they were oscillated continuously for about 10 h in an ultrasonic box with a working frequency of 25–40 kHz so that the nanoparticles can be uniformly dispersed. The oscillation time was a conference time and could ensure a full dispersion. It must be noted that no surfactant was added into the base liquid. In the study, the mass concentration of the nanofluids arranged from 0.2% to 2.0%.

The mass concentration w was used to describe the nanoparticles concentration, and the volume fraction θ can be estimated by following correlation:

$$\frac{1-w}{w}\cdot\frac{\rho_n}{\rho_0}=\frac{1-\theta}{\theta} \tag{1}$$

2.3. Experimental process

The test started after the nanofluid was filled into the CPL for a week. At the beginning of each test, the whole system was vacuumed to a pressure of 0.08 Pa before the charging of the working fluid. The experiment was carried out at the three steady operating temperatures of 30 °C, 40 °C and 55 °C, respectively. During each run, the temperature of the cooling water was carefully adjusted to keep the operating pressure at a stable state during each input. The temperature and the pressure were recorded by the data acquisition system only after the wall temperatures of the vapor line remained stable for a long time. The electric voltage and the current of the AC power supply were also recorded. After each run, the CPL was stopped from working for a week. After which the CPL was restarted again and the test was repeated. There was no meaningful difference between the two tests. The reason for the excellent repeatability should be that the random motion of nanoparticles in the base liquid under the effect of buoyancy could make the nanofluid uniform again after nanoparticles were settled for a long time. For a uniformly dispersed nanofluid, the experiment results could be well repeated.

The input power was calculated from the measured electronic voltage drop and the current and the heat flux was calculated according to the input power and the effective heated area of the evaporator. The average heat transfer coefficient of the evaporator (HTC), h, was calculated by the following equation:

$$h=\frac{q}{T_e-T_v} \tag{2}$$

The thermal resistance of the CPL, R, was calculated from Eq. (3):

$$R=\frac{T_e-T_c}{Q} \tag{3}$$

The experimental uncertainties of the heat flux and the HTC are given respectively as

$$\frac{\Delta q}{q}=\sqrt{\left(\frac{\Delta V}{V}\right)^2+\left(\frac{\Delta I}{I}\right)^2+\left(\frac{\Delta A}{A}\right)^2+\left(\frac{\Delta Q_{\text{loss}}}{Q_{\text{loss}}}\right)^2} \tag{4a}$$

$$\frac{\Delta h}{h}=\sqrt{\left(\frac{\Delta q}{q}\right)^2+\left(\frac{\Delta(\Delta T)}{\Delta T}\right)^2} \tag{4b}$$

To calculate the heat loss, the heat absorbed by the cooling water in the condenser and the heating power supplied to the evaporator were compared. The maximum heat loss was less than 3% of the input power. The maximum temperature uncertainty of the thermocouple was 0.2 K. Both the maximum uncertainties of the electric voltage drop and the current were the same 0.1%. The uncertainty caused by the heating area was 0.5%. Therefore, the uncertainties of the heat flux and the HTC were estimated to be 3.4% and 4.6%.

3. Experimental results and discussions

3.1. Determination of the optimal liquid filling ratio

Fig. 3(a) and (b) shows the effect of the filling ratio of both water and ethanol, which was defined as the ratio of the liquid volume to the whole volume of the CPL. The operating temperatures were fixed at 30 °C for water and 55 °C for ethanol, respectively. It is found from Fig. 3 that the thermal resistance is at the minimum when the filling ratio is about 55% either for water or for ethanol. For other operating temperatures, the present experiment has confirmed that the thermal resistances were also the least when the filling ratio was fixed at about 55%. Therefore, it could be concluded that there existed an optimal filling ratio to the CPL and this optimal filling ratio was about 55%.

3.2. Comparisons of the temperature distributions between water and the water based Cu nanofluids

Fig. 4(a) and (b) displays the temperature distributions of the evaporator wall, the vapor line, the condenser wall and the liquid line in the CPL using the base fluids and Cu nanofluids with a nanoparticle mass concentration of 1.0 wt% respectively. The filling ratio and the operating temperature were kept at 55% and 55 °C, respectively.

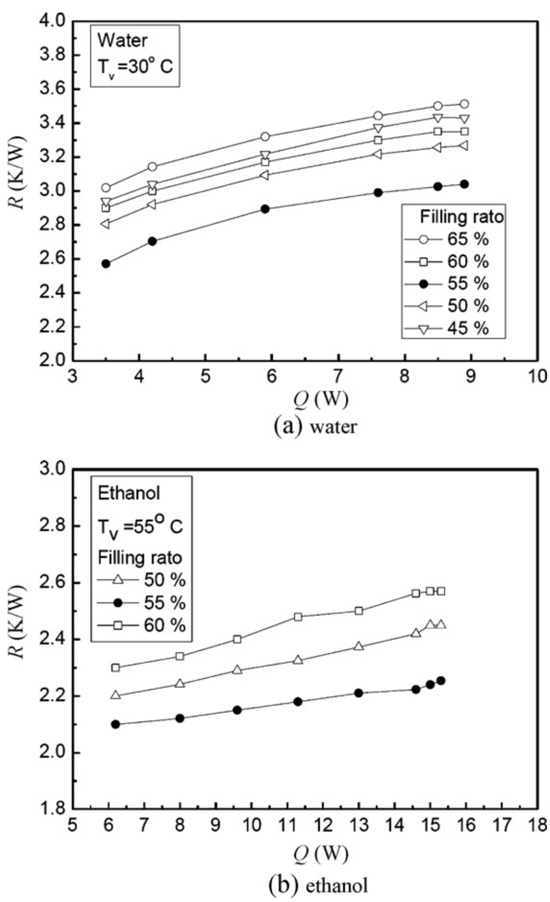

Fig. 3. Effect of the filling rate on the total thermal resistances of CPL using both water and ethanol.

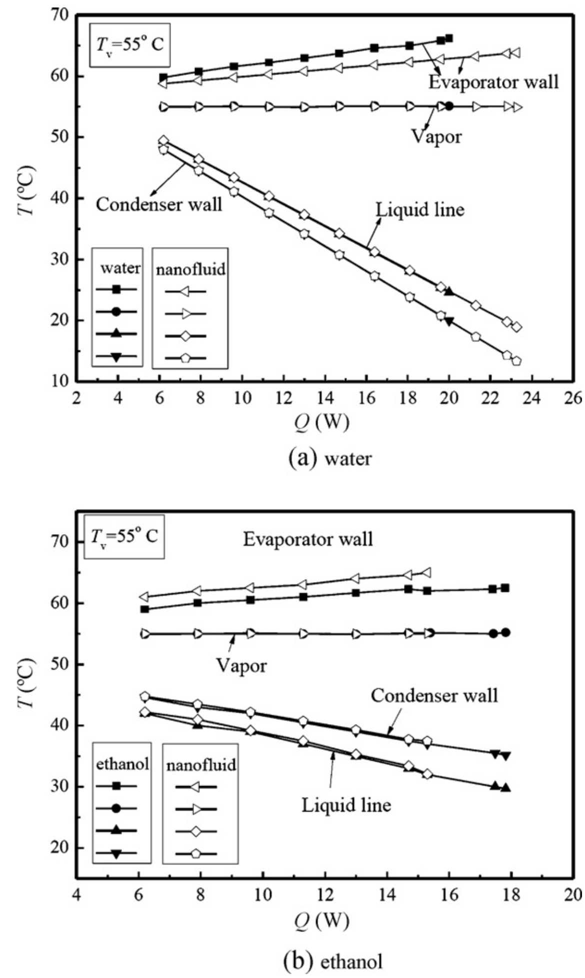

Fig. 4. Distributions of wall temperature in the CPL under the operating temperature of 55 °C.

For water as the working liquid, the wall temperatures of the evaporator for water are 59.8 °C and 65.8 °C when the input powers are fixed at 6.2 W and 19.6 W, respectively. While, for the water based Cu nanofluid as the working liquid, the wall temperatures of the evaporator are 58.4 °C and 62.4 °C at the same mentioned above input powers, respectively. This means that the wall temperatures of the evaporator for the nanofluid are lower than those for water at the same input power. The addition of nanoparticles in the working fluid reduces the wall temperature of the evaporator and enhances the heat transfer performance. The effect of nanoparticles on reducing the evaporator wall temperature is more significant at the high fluxes. In addition, the maximum input power is about 20 W for the CPL using water, while it goes up to 23.2 W for the CPL using the nanofluid. This result shows that the maximum heat removal capacity of the CPL is also improved when distilled water was replaced by the nanofluid.

For ethanol, similar to the case adding nanoparticles into water, the addition of nanoparticles in ethanol reduces also the wall temperature of the evaporator and increases the maximum heat removal capacity. The enhancement efficiency of the thermal performance is also basically the same extent as that for water.

On the other hand, after substituting the nanofluid for the base fluid, both condenser wall temperature and liquid temperature

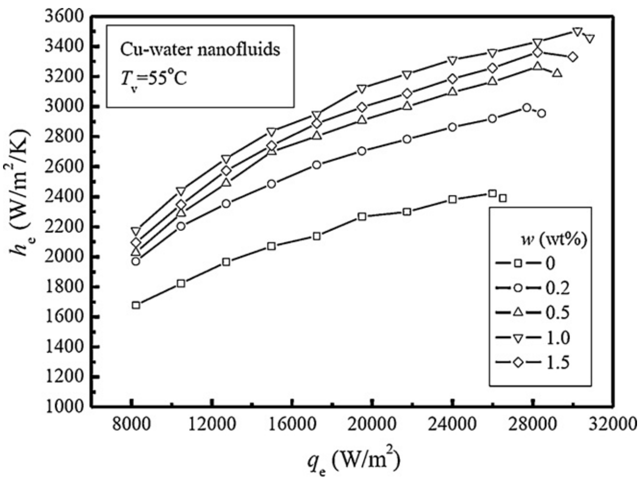

(a) Cu-water nanofluid

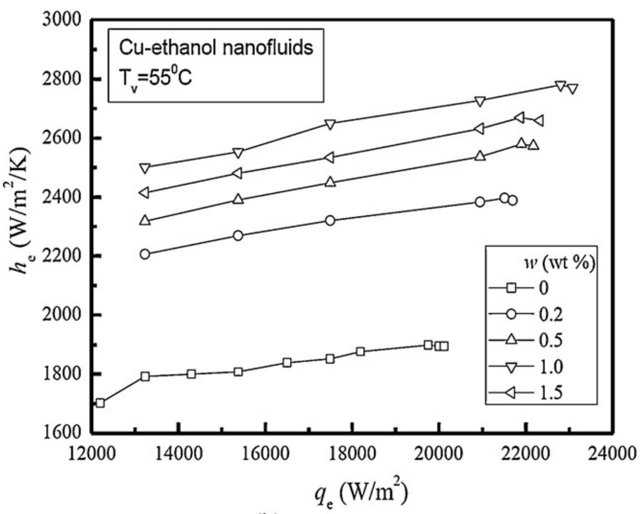

(b) Cu-ethanol nanofluids

Fig. 5. Effect of the nanoparticles mass concentration on the heat transfer coefficient in the evaporator.

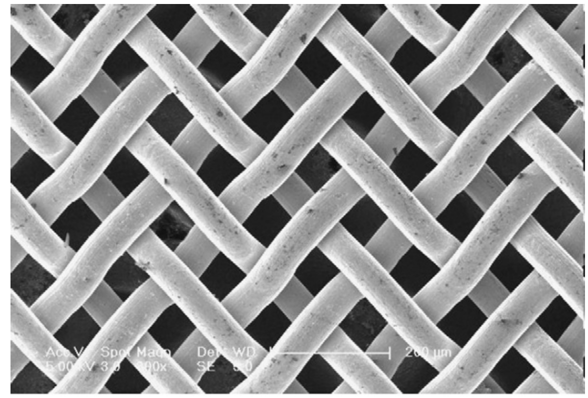
(a) mesh surface

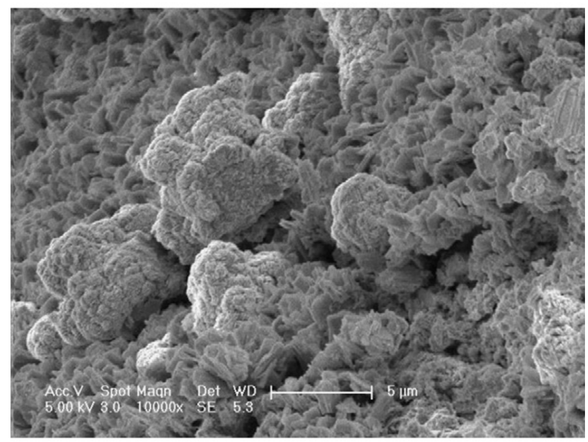

(b) heated surface

Fig. 6. The TEM photographs of the mesh and the heated surface after the test using the Cu-water nanofluid.

at the liquid line have hardly any changes. This fact means the nanofluid has no enhancement effect on the heat transfer in the condenser due to no nanoparticles passing through the condenser with vapor.

3.3. Effect of the mass concentration of nanoparticles on the heat transfer coefficients in the evaporator

Fig. 5(a) and (b) illustrates the effect of the nanoparticles mass concentration on the HTCs of the evaporator at the filling ratio of 55% for the water based nanofluid and the ethanol based nanofluid. The operating temperature was kept at 55 °C.

It is found that both the evaporating HTC and the maximum heat removal capacity of water are superior to those of ethanol due to that the surface tension and the thermal conductivity of water are all greater than those of ethanol. For every nanofluid tested, the HTC is increased with increasing the heat flux at low and moderate heat fluxes. Then, it decreases slowly at high heat fluxes. The maximum increases in the HTCs are about 38% and 45% compared with that of water and ethanol when the nanoparticles mass concentration is fixed at 1.0%. Additionally, the HTC increases with the addition of nanoparticles when the nanoparticles mass concentration is lower than 1.0%. Then it decreases to some extent when the nanoparticles mass concentration is larger than 1.0%. Therefore, it may be concluded that there exists an optimal mass concentration for both nanofluids which corresponds to the maximum enhancement effect. This optimal nanoparticles mass concentration is about 1.0% under all operating pressures in the present experiment. At the optimal mass concentration, both the HTC and the MHF of nanofluids are larger than those of the base fluids in the heat flux range tested.

Fig. 6(a) and (b) gives out transmission electronic microscope (TEM) photographs of the stainless mesh surface and the copper heated surface inside the CPL after the experiment using the water based nanofluid. It is clear from Fig. 6(a) that almost no sedimentation of nanoparticles is found on the mesh surface. On the other hand, it can also be clearly observed from Fig. 6(b) that there exists a very thin coating layer on the copper surface, and, the coating layer is a complicatedly porous structure. This fact indicates that the improvement of thermal performance of the CPL using nanofluids results mainly from the changes of the characteristics of working fluids and the sedimentation of nanoparticles on the heated surface.

The heat transfer enhancement of nanofluids inside the CPL evaporator may result from the following reasons: firstly, the increase of the effective thermal conductivity of the nanofluid; secondly, the decrease of the solid–liquid contact angle between the working fluid and the meshes. These two reasons result from the changes of nanofluid properties. Thirdly, the existence of the porous layer formed on the heated surface which also reduces the solid–liquid contact angle between the working fluid and the heated surface. The fourth may be attributed to the turbulence effect of the random motion (Brownian motion) of

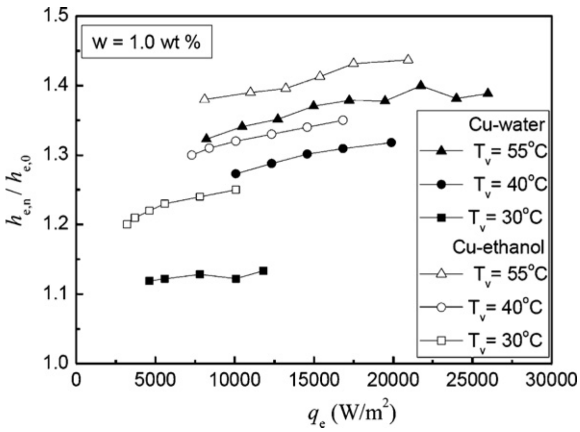

Fig. 7. Effect of operating temperature on the HTC enhancement ratio.

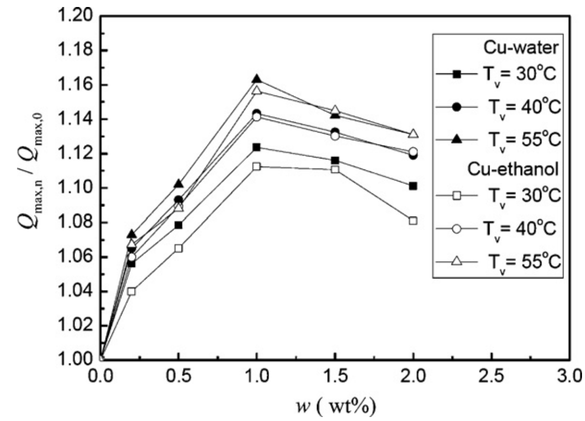

Fig. 8. Effect of operating temperature on the MHF enhancement ratio.

nanoparticles in the base liquid, which behaves as a nano-scale effect.

Reasons for the exiting an optimal concentration of nanoparticles in the CPL is similar to that in a micro-grooved heat pipe that has been estimated by some numerical simulations [23,27]. The capillary force inducted by the porous coating layer formed by nanoparticles on evaporation section will increase with increasing the nanoparticle concentration, and finally reaches a certain extent. Meantime, the liquid density, viscosity and flow drag will also increase with increasing the nanoparticle concentration. Therefore, there exists an optical nanoparticles concentration that keeps balance between the capillary force and the flow drag force.

3.4. Effects of operational temperature on both enhancement ratios of the HTC and the MHF

Fig. 7 reveals the effect of the operating temperature on the HTC enhancement ratio, which was defined as the ratio of the HTC of nanofluids to that of the base fluid at the same heat flux and operating temperature. The filling ratio and the nanoparticles mass concentration were kept respectively at 55% and 1.0 wt%. It is found that the HTC enhancement ratio increases with the increase of the operating temperature. The reason may be as explained as follows. The mode of heat transfer in the evaporator is a convective evaporation and the HTC increases with the increase of the effective thermal conductivity of the working liquid. Because the thermal conductivity of the nanofluid increases with the increase of the temperature, the HTC enhancement ratio will increase with increasing the temperature. In addition, the Brownian motion of nanoparticles would also increase with the increase of the temperature and this could also enhance the convective evaporation.

On the other hand, the HTC enhancement effect of the Cu-ethanol nanofluid is superior to that of the Cu-water nanofluid at all operating temperatures tested. The reason is unclear still in the present study stage.

Fig. 8 shows the effect of the operating temperature on the MHF enhancement ratio for both nanofluids, which was defined as the ratio of the MHF of the nanofluid to that of the base fluid. The filling ratio was fixed at 55%. Firstly, the MHF enhancement ratio increases rapidly when the nanoparticles mass concentration is lower than 1.0%, and then it decreases gradually when nanoparticles mass concentration is over 1.0%. It is also observed that the MHF enhancement ratio increases with the increase of the operating temperature. It should be noted that the kind of the base fluid has hardly any influence on the MHF enhancement ratio. The MHF of the nanofluids can increase up to 16% compared with that of the base fluids at the operating temperature of 55 °C.

The experiment mentioned above indicates that the thermal performance of the flat CPL with the evaporator heated from the bottom wall is improved with adding of Cu nanoparticles into the working liquid. In order to understand the influence of the heating location on the thermal performance of the CPL using nanofluids, a heat transfer test was carried out for the evaporator heated from the top wall. After the nanofluid was infused into the CPL, the CPL was undisturbed for a week, then, the experiment was carried out. No meaningful difference in the thermal performance was found after distilled water was substituted by nanofluids. The reason should be that the nanoparticles settled on the bottom wall of the evaporator cannot again come in the base liquid under the effect of the natural convection during heating process when the top wall was heated. The experimental result discovered that the heating location has great effect on the uniformity of nanofluids during the heating process, and then, has great effect on the performance improvement of the CPL using nanofluids.

Since no experimental data of the CPL using nanofluids can be applied to compare with the present CPL data, the experimental data from two cylindrical meshes wicked heap pipes using nanofluids [17,18] are compared with the present experimental data in this paper. Fig. 9 illustrates the compared result of the reducing ratio of the total thermal resistance of heat pipes using nanofluids among the existing experimental results of meshes wicked heat pipes. It is found from Fig. 9 that the reducing ratio of the total thermal resistance for the CPL is apparently lower than those of the cylindrical heat pipes proposed by Kang's study team [17] and slightly lower than those of the same cylindrical heat pipes proposed by Kang's

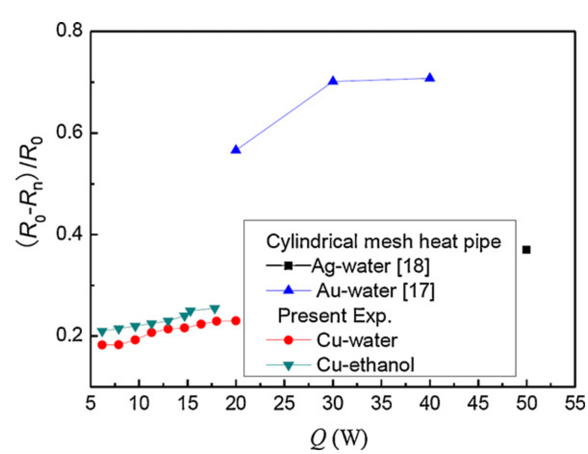

Fig. 9. Comparison of reducing rate of thermal resistances between CPL and mesh wicked heat pipes.

study team [18]. The reasons may mainly be that only the evaporation heat transfer is enhanced in the evaporator for the CPL and the evaporation and condensation heat transfer all are enhanced in the evaporator and condenser for the cylindrical meshes heat pipes.

4. Conclusions

An experimental research was carried out to investigate the thermal performance of a flat CPL using respectively the water based Cu nanofluids and the ethanol based Cu nanofluids as the working liquid. The evaporator was heated from the bottom wall. The conclusions are as follows:

(1) The wall temperatures of the evaporator for both nanofluids are lower than those for the base fluids. The addition of Cu nanoparticles into the base fluid can improve the thermal performance of the evaporator.
(2) The heat transfer coefficients of both nanofluids in the evaporator depend strongly on the nanoparticle mass concentration. There exists an optimal nanoparticles mass concentration which corresponds to the maximum heat transfer enhancement.
(3) The influences of the operating temperature on both enhancement ratios of the heat transfer coefficient and the maximum heat removal capacity are remarkable. Both the enhancement ratios of the heat transfer coefficient and the maximum heat removal capacity increase with the increase of the operating temperature. The heat transfer coefficients can be enhanced up to 38% and 45% after substituting the base fluids for Cu-water nanofluids. The maximum heat removal capacities can be enhanced up to 16% for nanofluids compared with those of the base fluids.

References

[1] J.F. Stenger, Experimental Feasibility Study of Water-filled Capillary-pumped Heat-transfer Loops, NASA TM-X-1310, Cleveland, 1966.
[2] K. Jentung, Overview of Capillary Pumped Loop Technology, ASME Heat Pipes and Capillary Pumped Loops, Atlanta, 1993.
[3] M. Maidanik, F. Yu, State-of-the-art of CPL and LHP technology, in: Proceeding of the 11th International Heat Pipe Conference, Tokyo, 1999.
[4] A. Faghri, Heat Pipe Science and Technology, 1st ed., Taylor & Francis Publishing Company, Washington, DC, 1995.
[5] T.H. Triem, K. Jentung, A. Tamara, O. Connell, Miniature loop heat pipes for electronic cooling, in: Proceeding of the IPACK2003 International Electronic Packaging Technical Conference and Exhibition, Hawaii, 2003.
[6] P.C. Chen, W.K. Lin, The application of capillary pumped loop for cooling of electronic components, Appl. Therm. Eng. 21 (2001) 1739–1754.
[7] C. Figus, L. Ounougha, P. Bonzom, W. Supper, C. Puillet, Capillary fluid loop developments in Astrium, Appl. Therm. Eng. 23 (2003) 1085–1098.
[8] I. Ramos, F.M. Vlassov, Experimental and theoretical investigation of a capillary pumped loop with a porous element in the condenser, Int. Commun. Heat Mass Transfer 25 (1998) 1085–1094.
[9] S.U.S. Choi, Enhancing thermal conductivity of fluids with nanoparticles, in: Proceedings of the 1995 ASME International Mechanical Engineering Congress and Exhibition, San Francisco, 1995.
[10] P. Keblinski, J.A. Eastman, D.G. Cahill, Nanofluids for thermal transport, Mater. Today 8 (2005) 36–44.
[11] Q.X. Wang, A.S. Mujumdar, Heat transfer characteristics of nanofluids: a review, Int. J. Therm. Sci. 46 (2007) 1–19.
[12] D. Weerapun, W. Somchai, A critical review of convective heat transfer of nanofluids, Renew. Sust. Energy Rev. 11 (2007) 797–817.
[13] M. Bahrami, M.M. Yovanovich, J.R. Culham, Assessment of relevant physical phenomena controlling thermal performance of nanofluids, in: Proceedings of 2006 ASME International Mechanical Engineering Congress and Exposition, Chicago, 2006.
[14] L.X. Cheng, F. Bandarra, P.E. Thome, R. John, Nanofluid two-phase flow and thermal physics: a new research frontier of nanotechnology and its challenges, J. Nanosci. Nanotechnol. 8 (2008) 3315–3332.
[15] D.S. Wen, G.P. Lin, S. Vafae, K. Zhang, Review of nanofluids for heat transfer applications, Particuology 7 (2009) 141–150.
[16] H.T. Chien, C.T. Tsai, P.H. Chen, P.Y. Chen, Improvement on thermal performance of a disk-shaped miniature heat pipe with nanofluids, in: IEEE Proceedings of the Fifth International Conference on Electronic Packaging Technology, Shanghai, China, 2003.
[17] W.C. Wei, S.H. Tsai, S.Y. Yang, S.W. Kang, Effect of nanofluids concentration on heat pipe thermal performance, IASME Trans. 2 (2005) 1432–1439.
[18] S.W. Kang, W.C. Wei, S.H. Tsa, S.Y. Yang, Experimental investigation of silver nano-fluid on heat pipe thermal performance, Appl. Therm. Eng. 26 (2006) 2377–2382.
[19] Z.H. Liu, J.G. Xiong, R. Bao, Boiling heat transfer characteristics of nanofluids in a flat heat pipe evaporator with micro-grooved heating surface, Int. J. Multiphase Flow 33 (2007) 1284–1295.
[20] Z.H. Liu, L. Lu, Thermal performance of axially micro-grooved heat pipe using carbon nanotube suspensions, J. Thermophys. Heat Transfer 23 (2009) 170–175.
[21] K.H. Do, S.P. Jang, Effect of nanofluids on the thermal performance of a flat micro heat pipe with a rectangular grooved wick, Int. J. Heat Mass Transfer 53 (2010) 2183–2192.
[22] X.F. Yang, Z.H. Liu, J. Zhao, Heat transfer performance of a horizontal micro-grooved heat pipe using CuO nanofluids, J. Micromech. Microeng. 18 (2008) 035038.
[23] C.Y. Tsai, H.T. Chien, P.P. Ding, B. Chan, T.Y. Luh, P.H. Chen, Effect of structural character of gold nanoparticles in nanofluids on heat pipe thermal performance, Mater. Lett. 58 (2004) 1461–1465.
[24] Y.T. Chen, W.C. Wei, S.W. Kang, C.S. Yu, Effect of nanofluids on flat heat pipe thermal performance, in: Proceedings of the 24th IEEE Semiconductor Thermal Measurement and Management Symposium, San Jose, 2008.
[25] R.R. Riehl, Analysis of loop heat pipe behaviour using nanofluid, in: Proceedings of Heat Powered Cycles International Conference (HPC), New Castle, 2006 (Paper 06102).
[26] S.W. Kang, W.C. Wei, S.H. Tsa, C.C. Huang, Experimental investigation of nanofluids on sintered heat pipe thermal performance, Appl. Therm. Eng. 29 (2009) 973–979.
[27] M. Shafahi, V. Bianco, K. Vafai, O. Manca, Thermal performance of flat-shaped heat pipes using nanofluids, Int. J. Heat Mass Transfer 53 (2010) 1438–1445.
[28] H.B. Ma, C. Wilson, B. Borgmeyer, K. Park, Q. Yu, S.U.S. Choi, T. Tirumala, Effect of nanofluids on the heat transport capability in an oscillating heat pipe, Appl. Phys. Lett. 88 (2006) 143116.1–143116.3.
[29] H.B. Ma, C. Wilson, K. Park, S.U.S. Choi, T. Tirumala, An experimental investigation of heat transport capability in a nanofluids oscillating heat pipe, J. Heat Transfer 128 (2006) 1213–1216.
[30] K. Park, H.B. Ma, Nanofluids effect on heat transport capability in a well-balanced oscillating heat pipe, J. Thermophys. Heat Transfer 21 (2007) 443–445.
[31] Y.H. Lin, S.W. Kang, H.L. Chen, Effect of silver nanofluids on pulsating heat pipe thermal performance, Appl. Therm. Eng. 28 (2008) 1312–1317.
[32] J. Li, D. Liang, K. Guo, R. Wang, S. Fan, Formation and dissociation of HFC134a gas hydrate in nano-copper suspension, Energy Convers. Manage. 47 (2006) 201–210.
[33] S.H. Noie, S.Z. Heris, M. Kahani, S.M. Nowee, Heat transfer enhancement using Al2O3/water nanofluid in a two-phase closed thermosyphon, Int. J. Heat Fluid Flow 30 (2009) 700–705.
[34] Z.H. Liu, X.F. Yang, G.S. Wang, G.L. Guo, Influence of carbon nanotube suspension on the thermal performance of a miniature thermosyphon, Int. J. Heat Mass Transfer 53 (2010) 1914–1920.
[35] H.S. Xue, J.R. Fan, Y.C. Hu, D.H. Hong, K.F. Cen, The interface effect of carbon nanotube suspension on the thermal performance of a two-phase closed thermosyphon, J. Appl. Phys. 100 (2006) 104909.1–104909.5.
[36] Z.H. Liu, X.F. Yang, G.L. Guo, Effect of nanoparticles in nanofluids on thermal performance in a miniature thermosyphon, J. Appl. Phys. 102 (2007) 013526.1–013526.8.
[37] S. Khandekar, Y.M. Joshi, B. Mehta, Thermal performance of closed two-phase thermosyphon using nanofluids, Int. J. Therm. Sci. 47 (2008) 659–667.
[38] P. Naphon, P. Assadamongkol, T. Borirak, Experimental investigation of titanium nanofluids on the heat pipe thermal efficiency, Int. Commun. Heat Mass Transfer 35 (2008) 1316–1319.
[39] P. Naphon, D. Thongkum, P. Assadamongkol, Heat pipe efficiency enhancement with refrigerant-nanoparticles mixtures, Energy Convers. Manage. 50 (2008) 772–776.